The Environmental Dependence of Galaxy Star Formation Rates

Within the widely-accepted cosmological framework, the mass density of the universe is dominated by cold dark matter. Protogalaxies are formed when normal baryonic gas falls into dark matter potential wells, cooling and forming stars at the centers of dark matter halos. These halos, along with their gaseous and stellar content, merge to form larger galaxies, which in turn merge to form groups, clusters, and filaments.

The buildup of stellar mass within this framework can be tested observationally through the evolution of the ultraviolet and near-infrared galaxy luminosity functions. The ultraviolet emission of galaxies is dominated by young, massive stars, and therefore permits measurements of the ongoing star formation rate (SFR). Near-infrared emission is dominated by old, low-mass stars, providing an indication of the amount of stars already formed. Deep *HST* imaging has formed the basis of much of the high redshift work in this area,[1–5] providing important constraints on the processes driving star formation. In particular, although standard, "quiescent" star formation models within a hierarchical framework can successfully reproduce local star formation rates, they underpredict the number of massive starforming galaxies at high redshift and the stellar mass already in place by a redshift of two.[6–9] Star formation models that include starbursts triggered by galaxy mergers have been more successful in matching the ultraviolet luminosity function at $z = 2 - 3$, but fail to produce enough stars at high redshift to match the infrared data at $z \sim 2$.[9,10] Recent models including starbursts from both galaxy mergers *and* encounters that do not lead to bound mergers (fly-by events) successfully reproduce both the ultraviolet and infrared data without altering the agreement with observations at low redshifts.[11]

In addition to the redshift dependence of star formation, there is growing observational evidence for an environmental dependence. In particular, star formation in the densest environments, namely galaxy clusters, appears to be suppressed in comparison to the field.[12–20] The suppression is strongest in cluster cores, with star formation increasing systematically with increasing distance from the cluster center. Recent studies involving large samples of galaxies at low redshift have provided important clues as to which mechanisms drive the SFR-density relation.[21,22] First, these studies reveal that the suppression of SFR persists at relatively low densities and large distances from clusters, where cluster-specific processes are not important. Second, the star formation properties of galaxies appear to be more dependent upon the large-scale (5 Mpc) density than they are upon the mass of the group or cluster in which they are embedded.[23] The former is closely linked to the formation time of a galaxy, while the latter is linked to current processes within the group or cluster. The observations imply that the star formation properties of galaxies are more closely tied to *when* a galaxy formed, rather than *current* environmental effects. Third, these observations reveal that suppressed regions contain a lower fraction of starforming galaxies, rather than galaxies with systematically lower SFRs compared to the field. This fact is evidence against models in which the environment induces a slow decrease in a galaxy's SFR.

A proper treatment of starbursts associated with galaxy mergers and fly-by events can reproduce the observed evolution of star formation within galaxies. Can it also reproduce the observed environmental dependence of star formation? Galaxies presently found in high

density environments may have undergone more interactions in the distant past. Galaxies have access to only a limited supply of gas from which to form stars, and thus those that have undergone multiple interactions may quickly exhaust their gas reservoir, leading to a decline in SFR. Although galaxy-galaxy interactions at high redshift could plausibly result in the observed relationship between SFR and density observed in the local universe, it is a scenario that has yet to be tested in detail. The first goal of this proposal is to perform such a test using existing dark matter simulations in combination with simple models that treat starbursts due to both mergers and fly-by events. My approach is described in greater detail in the next section.

In the scenario described above, the present-day SFR-density relation is the result of interactions at an early epoch, before the galaxies are incorporated into larger structures. In this case, the threshold local galaxy density at which SFRs begin to correlate with environment should systematically increase with decreasing redshift. In contrast, if instead the SFR of a galaxy depends on its current local environment, but not its interaction history, the threshold density should remain constant with redshift. Quality observations at high redshift offer the best opportunity for measuring the evolution of the SFR-density relation, thereby discriminating between these models. The second goal of my proposed program is to make such observations, described in detail in the final section.

Theoretical Program: Modelling Starbursts in Simulations

In the simulation I propose to utilize, the dark matter halos of galaxies within a 70 Mpc box are represented by 80 million particles.[24] This simulation is able to resolve galaxies smaller than the Magellanic Clouds down to the center of galaxy clusters. The final output contains tens of thousands of halos, so I will be able to achieve a statistical significance similar to the largest existing observational studies.[23]

I will model quiescent star formation using procedures developed in standard semi-analytic models of galaxy formation.[25–27] In these models, star formation is driven by both the cooling of hot gas and by the refueling of cold gas during mergers. In addition to this quiescent mode of star formation, I will model the starbursts associated with galaxy mergers and fly-by events following the derivation of the fraction of cold gas destabilized by encounters put forth by Cavaliere and Vittorini.[11,28] The spectral energy distribution (SED) of a galaxy can be modelled by convolving the SFR with the SED of a single-aged stellar population.[29] I will compare the resulting dependence of SFR with observations[21–23] of local galaxies, "observing" the simulation with a suitable projection of positions and velocities in order to mimic the procedure adopted by observers.

In addition to its redshift and environmental dependences, star formation depends upon galaxy mass. The average starforming galaxy was more massive in the past, an effect known as *cosmic downsizing*.[30,31] This effect has also been observed in clusters, which show evidence of luminous post-starburst galaxies at intermediate redshifts that are absent in the nearby Coma cluster.[32] The most straightforward explanation is that the mass of actively starforming galaxies falling into clusters decreases at low redshifts. Can we understand downsizing in the context of galaxy-galaxy interactions? If high mass galaxies have on average undergone more interactions, they may have depleted all of their gas by the current epoch, while low mass galaxies have not. The simulation described above will allow me to explore the connection between interaction history and galaxy mass and how such a connection might explain cosmic downsizing.

Observational Program: Star Formation Rates at High Redshift

Past studies of the SFR in distant galaxies suffer from two limitations which prevent their use in measuring the SFR-environment correlation. First, they have not included low-density regions. Second, they commonly utilize [OII] emission lines to measure the SFR. Although it is easily detectable at high redshift ($z \sim 1$), [OII] is not an ideal diagnostic for SFR.[33,34] The strength of the [OII] 3727λ line is not directly coupled to the ionizing luminosity of young stars, and it is sensitive to variations in the metallicity and the ionization state of the gas. More importantly, it is strongly affected by dust.[35–40] Past studies may therefore have a highly biased view of the SFRs in distant galaxies. For example, several spectroscopic surveys of distant clusters[12,14,41–43] have revealed a population of galaxies with spectra displaying strong Balmer absorption but lacking emission lines. These objects have been interpreted as galaxies that are not currently forming stars, but have recently undergone a starburst.[12,14] If this interpretation is correct, the starforming progenitors of these post-starburst galaxies have yet to be identified.[17] An alternate interpretation is that they are galaxies in which star formation is totally obscured at optical wavelengths.[37]

My observational plan is designed to remedy both of these problems. I will map the SFR out to the low density regions ($6R_{\rm virial}$) surrounding CL1216, one of the clusters I have been studying as part of an *HST/ACS* survey of ten $z \sim 0.8$ clusters (see Figure 1). I will use mid- to far-infrared data obtainable with *SIRTF* to calculate robust SFRs that are unaffected by dust. My proposed *SIRTF* observations, including overheads, can be completed in 9 hours, well within the time for a reasonable program. I will simultaneously measure redshifts and [OII] line strengths using the Deep Extragalactic Imaging Multi-Object Spectrograph (*DEIMOS*), installed on Keck II. Accounting for observational overheads, in two nights I can spectroscopically confirm ∼600 galaxies that are both near the cluster redshift and within ∼6 virial radii of CL1216.

The proposed observations nicely complement other works in progress. In particular, Treu et al.[44] are conducting an optical spectroscopic survey of galaxies up to 5 Mpc from the center of CL0024+16 at z=0.4, for which they already have complementary *HST/WFPC2* imaging. Their study provides an intermediate redshift sample, in addition to the zero redshift baseline discussed in the introduction, with which to compare my high redshift results. In particular, my proposed optical spectroscopy will yield [OII]-derived SFRs, which can be compared directly with those measured at z=0.4.

The DEEP2 survey will also return a wealth of information on the star formation properties of galaxies at $z \sim 1$.[45] One of their survey fields, the Groth Strip, will be particularly well-studied, with mid- to far-infrared data from *SIRTF*, *HST* imaging, groundbased *BRI* imaging, and X-ray data. My proposed data set will be of similar quality and wavelength coverage, but for a region surrounding a rich cluster. This new dataset will allow a fair comparison between cluster and field environments at similar redshifts.

Strategy for Proposed *SIRTF* Observations

The Multiband Imaging Photometer for *SIRTF* (*MIPS*) simultaneously collects mid- to far-infrared data at three narrow bandpasses centered at 24 μm, 72 μm, and 160 μm. Studying a sample of 156 local galaxies, Papovich et al. (2002)[46] found that the total infrared fluxes (8–1000 μm) of $z \sim 1$ galaxies can be constrained to within a factor of 2.5 using 24 μm *MIPS* data. We therefore optimize our observations for the 24 μm band, while keeping in mind that

the addition of 70 μm data will help to improve this constraint by a factor of $\lesssim 6$.

In a study of three clusters at z=0.76, z=0.9, and z=0.92, Postman et al. (2001)[18] used [OII] to measure the mean SFRs of cluster members as a function of redshift. Interpolating their results, I expect a mean [OII]-derived SFR of 1.5 $M_\odot yr^{-1}$ for cluster members at z=0.8, and higher values in the surrounding regions. The ratio between IR-derived SFRs and [OII]-derived SFRs has been found to range from 10–100.[40] Thus, I expect an average IR-derived SFR of more than 15 $M_\odot yr^{-1}$. In order to ensure high signal-to-noise photometry on galaxies with SFRs significantly below this average, I have calculated the exposure time necessary to detect a galaxy forming stars at a rate 15 times smaller than this average.

According to Bell (2003),[47] a SFR of 1 $M_\odot yr^{-1}$ corresponds to a total IR luminosity of $\log_{10}(L_{TIR}/L_\odot) \sim 9.8$. The flux in the 24 μm band is typically a factor of $0.16 L_{TIR}$.[46] Thus, in order to detect galaxies with SFRs as low as 1 $M_\odot yr^{-1}$, our IR data must be sensitive to fluxes as low as $\log_{10}(L_{24\mu m}/L_\odot) \sim 9$. Assuming the concordance cosmology, an object at this luminosity at $z = 0.8$ would have a flux of $F_{24\mu m} \sim 50$ μJy. Galaxies smaller than 15" (113 kpc at z=0.8) will be spatially unresolved in the 24 μm *MIPS* band. Using SPOT, we estimate that the background in the field of CL1216 falls in the "medium" category. The integration time required for a 1σ detection of a 50 μJy point source with a medium background is ∼400 seconds[1]. Because L_{TIR} is a steep function of SFR, the signal-to-noise ratio (SNR) increases quickly with SFR. A 400 second exposure time will therefore provide adequate SNRs for galaxies forming stars well below the average expected IR-derived rate of 15 $M_\odot yr^{-1}$ (see Figure 2). Although both the expected flux and sensitivity are higher at 70 μm, local confusion will limit its utility[2]. I therefore expect to have usable 70 μm data for a bright subset of the galaxies detected at 24 μm.

Since I wish to cover a relatively large area of the sky (0.5°× 0.5°), I will use the *MIPS* Scan Map AOT. The exposure time per pixel resulting from a single scan at a medium scan rate is 40 seconds at both 24 μm and 70 μm. A single map cycle consisting of 6 scan legs with a cross scan step of 302" (minimal overlap) and scan length of 0.5 degrees should cover the desired area with an exposure time of 40 seconds per pixel (see Figure 3). In order to attain a total exposure time of 400 seconds per pixel, I propose 3 AORs consisting of 3 map cycles each and 1 AOR consisting of just 1 map cycle. Using SPOT, I estimate that this program, including overheads, can be executed in (3 × 161 min) + 56 min = 539 min ∼ 9 hours.

Strategy for Proposed *DEIMOS* Observations

Because of its high throughput and its ability to take spectra of 140 objects simultaneously, *DEIMOS* is the ideal instrument with which to execute my spectroscopic program. Based upon spectra the EDisCS collaboration has already obtained for galaxies in the center of CL1216, I need 1 hour to acquire spectra with signal to noise suitable for redshift and [OII] linewidth determination. *DEIMOS* has a $9' \times 9'$ field of view. Thus, in 9 hours, I can tile the 0.5°× 0.5° area around CL1216. Using photometric redshift pre-selection, $\gtrsim 50\%$ of spectroscopic targets should lie within the redshift range in which I am interested. Thus, accounting for observational overheads I could spectroscopically confirm ∼600 galaxies within both my target redshift range and ∼6 virial radii of CL1216 in less than two nights.

[1] `http://sirtf.caltech.edu/SSC/mips/sensmedgifs/24scanmed.gif`

[2] `http://sirtf.caltech.edu/SSC/mips/sensmedgifs/70scanmed.gif`

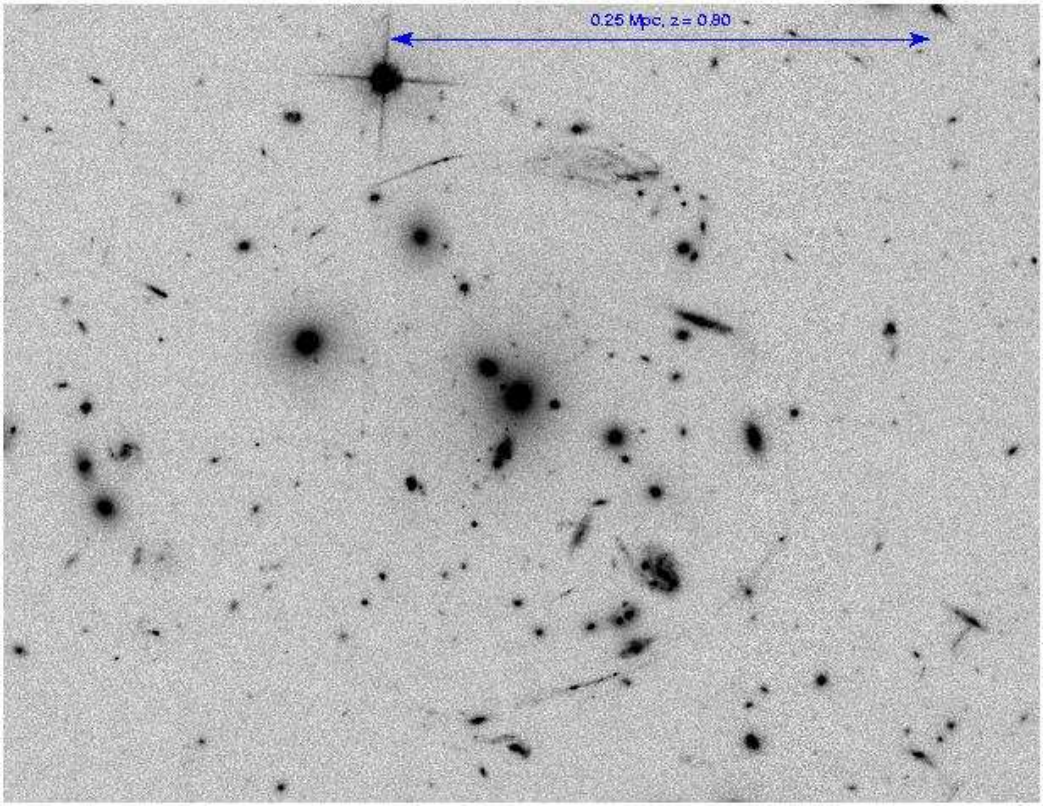

Figure 1: The image at left shows a ∼0.43 Mpc × 0.56 Mpc region around the center of CL1216, imaged in *F814W* with the *ACS/WFC* on board the *HST*. CL1216 is one of the high redshift clusters from the ESO Distant Cluster Survey (EDiSCS). The EDiSCS collaboration, of which I am a member, has collected an extensive data set for the inner 1.5 Mpc × 1.5 Mpc region of the cluster, including groundbased *BVRIK* imaging, *F814W HST/ACS* imaging, and optical spectroscopy. A larger 13.5 Mpc × 13.5 Mpc region around the cluster has been imaged in *VRI* (sufficient for photometric redshift estimation) and in the X-ray with *XMM-Newton*. Our proposed observations would add *SIRTF* mid- to far-infrared data as well as *DEIMOS* spectroscopy in this larger region.

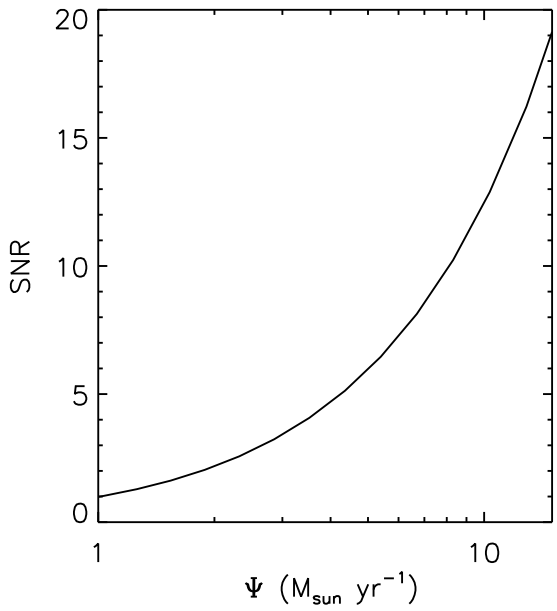

Figure 2: Signal-to-noise ratio (SNR) expected in the 24 μm band, as a function of SFR. The average IR-derived SFR for cluster members is expected to be 15 $M_{\odot}yr^{-1}$, where the plot cuts off.

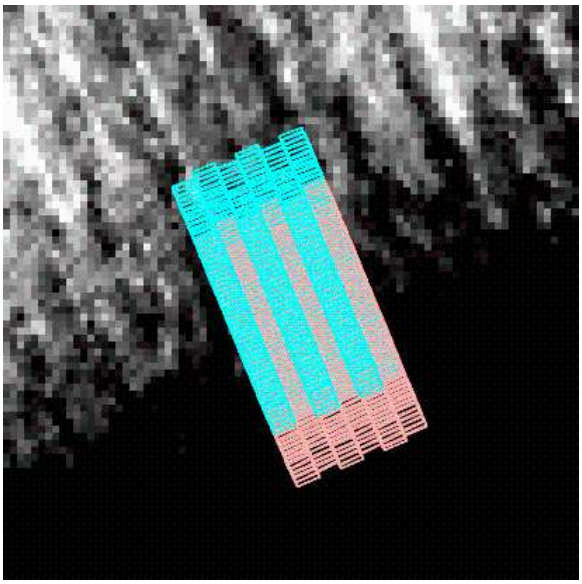

Figure 3: SPOT-generated visualization of the proposed 24 μm (turquoise) and 70 μm (pink) *MIPS* observations overlaid on a 2° × 2° ISSA image of a field centered on CL1216. This figure is available in color at `http://www.astro.washington.edu/desai/SIRTF`.

References

1. J. G. Cohen, R. Blandford, D. W. Hogg, M. A. Pahre, and P. L. Shopbell 1999, *ApJ* 512, 30–47.
2. J. G. Cohen 2002, *ApJ* 567, 672–701.
3. P. Madau, H. C. Ferguson, M. E. Dickinson, M. Giavalisco, C. C. Steidel, and A. Fruchter 1996, *MNRAS* 283, 1388–1404.
4. P. Madau, L. Pozzetti, and M. Dickinson 1998, *ApJ* 498, 106–+.
5. C. C. Steidel, K. L. Adelberger, M. Giavalisco, M. Dickinson, and M. Pettini 1999, *ApJ* 519, 1–17.
6. A. Fontana, N. Menci, S. D'Odorico, E. Giallongo, F. Poli, S. Cristiani, A. Moorwood, and P. Saracco 1999, *MNRAS* 310, L27–L32.
7. A. Fontana, F. Poli, N. Menci, M. Nonino, E. Giallongo, S. Cristiani, and S. D'Odorico 2003, *ApJ* 587, 544–550.
8. L. Pozzetti, A. Cimatti, G. Zamorani, E. Daddi, N. Menci, A. Fontana, A. Renzini, M. Mignoli, F. Poli, P. Saracco, T. Broadhurst, S. Cristiani, S. D'Odorico, E. Giallongo, and R. Gilmozzi 2003, *A&A* 402, 837–848.
9. A. Cimatti, L. Pozzetti, M. Mignoli, E. Daddi, N. Menci, F. Poli, A. Fontana, A. Renzini, G. Zamorani, T. Broadhurst, S. Cristiani, S. D'Odorico, E. Giallongo, and R. Gilmozzi 2002, *A&A* 391, L1–L5.
10. R. S. Somerville, J. R. Primack, and S. M. Faber 2001, *MNRAS* 320, 504–+.
11. N. Menci, A. Cavaliere, E. Fontana, E. Giallongo, F. Poli, and V. Vittorini 2003, *in preparation* .
12. W. J. Couch and R. M. Sharples 1987, *MNRAS* 229, 423–456.
13. R. G. Abraham, T. A. Smecker-Hane, J. B. Hutchings, R. G. Carlberg, H. K. C. Yee, E. Ellingson, S. Morris, J. B. Oke, and M. Rigler 1996, *ApJ* 471, 694–+.
14. B. M. Poggianti, I. Smail, A. Dressler, W. J. Couch, A. J. Barger, H. Butcher, R. S. Ellis, and A. J. Oemler 1999, *ApJ* 518, 576–593.
15. M. L. Balogh, S. L. Morris, H. K. C. Yee, R. G. Carlberg, and E. Ellingson 1999, *ApJ* 527, 54–79.
16. M. L. Balogh and S. L. Morris 2000, *MNRAS* 318, 703–714.
17. W. J. Couch, M. L. Balogh, R. G. Bower, I. Smail, K. Glazebrook, and M. Taylor 2001, *ApJ* 549, 820–831.
18. M. Postman, L. M. Lubin, and J. B. Oke 2001, *AJ* 122, 1125–1150.
19. M. L. Balogh, W. J. Couch, I. Smail, R. G. Bower, and K. Glazebrook 2002, *MNRAS* 335, 10–22.
20. K. A. Pimbblet, I. Smail, T. Kodama, W. J. Couch, A. C. Edge, A. I. Zabludoff, and E. O'Hely 2002, *MNRAS* 331, 333–350.
21. I. Lewis, M. Balogh, R. De Propris, W. Couch, R. Bower, A. Offer, J. Bland-Hawthorn, I. K. Baldry, C. Baugh, T. Bridges, R. Cannon, S. Cole, M. Colless, C. Collins, N. Cross, G. Dalton, S. P. Driver, G. Efstathiou, R. S. Ellis, C. S. Frenk, K. Glazebrook, E. Hawkins, C. Jackson, O. Lahav, S. Lumsden, S. Maddox, D. Madgwick, P. Norberg, J. A. Peacock, W. Percival, B. A. Peterson, W. Sutherland, and K. Taylor 2002, *MNRAS* 334, 673–683.
22. P. L. Gómez, R. C. Nichol, C. J. Miller, M. L. Balogh, T. Goto, A. I. Zabludoff, A. K. Romer, M. Bernardi, R. Sheth, A. M. Hopkins, F. J. Castander, A. J. Connolly, D. P. Schneider, J. Brinkmann, D. Q. Lamb, M. SubbaRao, and D. G. York 2003, *ApJ* 584, 210–227.
23. M. Balogh, V. Eke, C. Miller, I. Lewis, R. Bower, W. Couch, R. Nichol, and J. Bland-Hawthorn 2003, *in preparation* .
24. D. Reed, J. Gardner, T. Quinn, J. Stadel, M. Fardal, G. Lake, and F. Governato 2003, `astro-ph/0301270` .
25. R. S. Somerville and J. R. Primack 1999, *MNRAS* 310, 1087–1110.
26. S. Cole, C. G. Lacey, C. M. Baugh, and C. S. Frenk 2000, *MNRAS* 319, 168–204.
27. N. Menci, A. Cavaliere, A. Fontana, E. Giallongo, and F. Poli 2002, *ApJ* 575, 18–32.
28. A. Cavaliere and V. Vittorini 2000, *ApJ* 543, 599–610.
29. G. Bruzual and S. Charlot 2003, *MNRAS* 344, 1000–1028.
30. L. L. Cowie, A. Songaila, and A. J. Barger 1999, *AJ* 118, 603–612.
31. G. Kauffmann, T. M. Heckman, S. D. M. White, S. Charlot, C. Tremonti, E. W. Peng, M. Seibert, J. Brinkmann, R. C. Nichol, M. SubbaRao, and D. York 2003, *MNRAS* 341, 54–69.
32. B. M. Poggianti, T. J. Bridges, Y. Komiyama, M. Yagi, D. Carter, B. Mobasher, S. Okamura, and N. Kashikawa 2003, `astro-ph/0309449` .
33. R. A. Jansen, M. Franx, and D. Fabricant 2001, *ApJ* 551, 825–832.
34. S. Charlot and M. Longhetti 2001, *MNRAS* 323, 887–903.
35. A. W. Blain, I. Smail, R. J. Ivison, and J.-P. Kneib 1999, *MNRAS* 302, 632–648.
36. H. Flores, F. Hammer, T. X. Thuan, C. Césarsky, F. X. Desert, A. Omont, S. J. Lilly, S. Eales, D. Crampton, and O. Le Fèvre 1999, *ApJ* 517, 148–167.
37. I. Smail, G. Morrison, M. E. Gray, F. N. Owen, R. J. Ivison, J.-P. Kneib, and R. S. Ellis 1999, *ApJ* 525, 609–620.
38. B. M. Poggianti and H. Wu 2000, *ApJ* 529, 157–169.
39. D. Fadda, D. Elbaz, P.-A. Duc, H. Flores, A. Franceschini, C. J. Cesarsky, and A. F. M. Moorwood 2000, *A&A* 361, 827–840.
40. P.-A. Duc, B. M. Poggianti, D. Fadda, D. Elbaz, H. Flores, P. Chanial, A. Franceschini, A. Moorwood, and C. Cesarsky 2002, *A&A* 382, 60–83.
41. D. G. Fabricant, J. E. McClintock, and M. W. Bautz 1991, *ApJ* 381, 33–54.
42. D. Fisher, D. Fabricant, M. Franx, and P. van Dokkum 1998, *ApJ* 498, 195–+.
43. A. Dressler, I. Smail, B. M. Poggianti, H. Butcher, W. J. Couch, R. S. Ellis, and A. J. Oemler 1999, *ApJS* 122, 51–80.
44. T. Treu, R. S. Ellis, J. Kneib, A. Dressler, I. Smail, O. Czoske, A. Oemler, and P. Natarajan 2003, *ApJ* 591, 53–78.
45. M. Davis, S. M. Faber, J. Newman, A. C. Phillips, R. S. Ellis, C. C. Steidel, C. Conselice, A. L. Coil, D. P. Finkbeiner, D. C. Koo, P. Guhathakurta, B. Weiner, R. Schiavon, C. Willmer, N. Kaiser, G. A. Luppino, G. Wirth, A. Connolly, P. Eisenhardt, M. Cooper, and B. Gerke 2003 in *Proceedings of the SPIE*, 4834, 161–172.
46. C. Papovich and E. F. Bell 2002, *ApJ* 579, L1–L4.
47. E. F. Bell 2003, *ApJ* 586, 794–813.